VICTORIA UNIVERSITY
MELBOURNE AUSTRALIA

Cyclization of PLP 139-151 peptide reduces its encephalitogenic potential in experimental autoimmune encephalomyelitis

This is the Accepted version of the following publication

Cyclization of PLP$_{139-151}$ peptide reduces its encephalitogenic potential in experimental autoimmune encephalomyelitis

Athanasios Lourbopoulos [a,b], Minos-Timotheos Matsoukas [c], Maria Katsara [d], George Deraos [e,f], Aggeliki Giannakopoulou [a], Roza Lagoudaki [a], Nikolaos Grigoriadis [a], John Matsoukas [f,*], Vasso Apostolopoulos [g,*]

[a] *B' Department of Neurology, Laboratory of Experimental Neurology and Neuroimmunology, AHEPA University Hospital, Aristotle University of Thessaloniki, 54636, Greece.*
[b] *Institute for Stroke and Dementia Research, Klinikum der Universität München, Ludwig Maximilian University (LMU), Munich, 81377, Germany.*
[c] *Department of Pharmacy, University of Patras, Patras 26500, Greece*
[d] *Novartis (Hellas) SACI, Medical Department, National Road No1 (12th Km). GR-144 51, Metamorphosis-Athens, Greece*
[e] *Department of Chemistry, University of Patras, Patras 26500, Greece*
[f] *Eldrug, Patras Science Park, Patras, Greece*
[g] *Centre for Chronic Disease, College of Health and Biomedicine, Victoria University, VIC 3030, Australia*

Running Title: Cyclic PLP$_{139-151}$ ameliorates EAE

_____

Abbreviations: AI, axonal injury; AL, axonal loss; CFA, complete Freund's adjuvant; cPLP, cyclic PLP$_{139-151}$ peptide; CNS, central nervous system; EAE, experimental autoimmune encephalomyelitis; HLA, human leukocyte antigen; linPLP, linear PLP$_{139-151}$ peptide; MHC, major histocompatibility complex; MHC, major histocompatibility complex; MS, multiple sclerosis; PLP, proteolipid protein; TCR, T cell receptor

* Corresponding Authors:
  Email address: vasso.apostolopoulos@vu.edu.au (V. Apostolopoulos),
                       imats1953@gmail.com (J. Matsoukas)

Senior Authors: Vasso Apostolopoulos, John Matsoukas

ABSTRACT

_____

We report the novel synthesis of cyclic $PLP_{139-151}$ (cPLP) and its application in SJL/J mice to study its encephalitogenic effects. Our results indicate that the cPLP analog is minimally encephalitogenic when administered to induce experimental autoimmune encephalomyelitis (low disease burden, minimal inflammatory, demyelinating and axonopathic pathology compared to its linear counterpart). Proliferation assays confirmed the low stimulatory potential of the cPLP compared to linPLP (2.5-fold lower proliferation) as well as inducing lower antibody responses. Molecular modeling showed a completely different TCR recognition profile of cPLP in regard to linPLP, where H^{147} replaces W^{144} and F^{151}-K^{150} replace H^{147} as TCR contacts, which may explain the difference on each peptide's response.

_____

1. Introduction

Experimental autoimmune encephalomyelitis (EAE) is an experimental model of demyelination, inflammatory processes and axonopathy within the central nervous system (CNS) of susceptible animals, using the triggering of various CNS antigens such as myelin basic protein (MBP), proteolipid protein (PLP) and myelin oligodendrocyte glycoprotein (MOG) or their peptides [1]. Due to the similarities of EAE with multiple sclerosis (MS), this model is widely used to study pathological mechanisms as well as novel experimental treatments for the disease [2-4]. Peptides PLP_{40-70}, $PLP_{100-119}$, $PLP_{178-191}$ and $PLP_{139-151}$ are the major encephalitogenic epitopes in the mouse strain SJL/J (I-A^s) [5-7]. Both of $PLP_{178-191}$ and $PLP_{139-151}$ peptides bind with similar affinity to major histocompatibility (MHC) class II (MHC-II; I-A^s), although, $PLP_{139-151}$ elicits stronger immune responses and EAE in SJL/J mice [6].

The peptides that induce EAE bear different immunogenic properties in each animal species which is largely determined by the specific properties of the major histocompatibility complex (MHC)-II haplotype of the animal. Specific peptide motifs within the antigen-binding groove of the MHC complex determines the affinity to the antigen and subsequent T-cell receptor (TCR) recognition and activation of the cell [8]. This MHC-antigen-TCR trimolecular complex is the key step to induce EAE with antigenic peptides and is possibly a key factor to MS immune-pathology [9, 10]. In fact, a number of immunotherapeutic strategies are based on blocking the formation of this complex, such as, anti-MHC-II antibodies or anti-CD4 antibodies which consequently suppress EAE [11-13]. In addition, any modification to the antigenic peptide, and any caused deviation from a tight MHC-antigen-TCR match can lead to reduced T-cell activation and different profiles of secreted cytokines.

Based on this concept, there have been several attempts to alter the trimolecular complex affinities and render autoreactive T-cells in MS and EAE inactive or eliminated. This approach of altered peptide ligands (APL; 1-2 amino acid modifications within a peptide) have resulted in immunomodulation of immune responses from pro- to anti-inflammatory. In fact, we have shown that 1-2 amino acid mutations to MBP peptide induces anti-inflammatory cytokines, which can be further diverted from T helper (Th)-1 to Th2 when conjugated to a novel carrier mannan [14-22]. Likewise, substitution of the TCR binding amino acids at positions 144 (Tryptophan, W) and 147 (Histidine, H) to L^{144} and R^{147} was able to antagonise T cell clones specific for $PLP_{139-151}$ epitope, block the induction of EAE and prevent progression of EAE [3, 16, 23, 24]. An alternative approach was recently published, whereby non-peptide mimetics of MBP_{83-96} T cell epitope can function as TCR antagonists by the inclusion of compounds obtained through the ZINC database [25]. Hence such an approach may pave the way to developing alternative and improved immunotherapeutics against MS [25].

Using alternative approaches to altering the tight interaction of the trimolecular complex, we recently showed that cyclic MOG_{35-55} peptide had a significant lower immunogenic potential in appropriate recipient animals (C57BL/6 mice), due to reduced affinity to MHC-II alleles [26]. In the present study we studied the immunogenic properties of novel synthesized cyclic (head to tail) $PLP_{139-151}$ peptide (cyclo(139-151)$PLP_{139-151}$; cPLP), using our previous successfully established process [26]. By keeping the same antigenic linear epitope of $PLP_{139-151}$ (linPLP) that induces EAE in SJL/J mice and changing the sterotaxy of the molecule to a cyclic one (cPLP), we tested the *in vivo* immunogenic and encephalitogenic potential of the

specific cPLP and linPLP peptides in SJL/J mice. Additionally, we determined the interactions of the cPLP peptide compared to linPLP counterpart in complex with MHC-II (H-2 IA^s) using appropriate *in silico* binding and structural studies (docking and homology modelling).

2. Results and discussion

Immunotherapeutic strategies have involved APL of peptide constituents of the myelin sheath (MBP, PLP and MOG) that are able to modulate/divert immune responses from pro-inflammatory (Th1) to anti-inflammatory (Th2) [18]. We recently demonstrated for the first time in a different mouse model (C57BL/6) that cMOG$_{35-55}$ peptide was able to significantly ameliorate clinical disease and underlying pathology when co-administered with encephalitogenic linear MOG$_{35-55}$ peptide, in both acute and chronic phases of EAE [26]. Herein, we showed, in the SJL/J mouse model that cyclization (cPLP) of the encephalitogenic linPLP peptide alters histopathological outcomes and disease severity of EAE in mice. Such cyclic modifications of linear peptides may provide novel immunomodulatory approaches for the future against MS [27].

2.1. Cyclic PLP is only minimal encephalitogenic compared to its linear analog

Animals of the control group developed a single-relapse EAE with a residual clinical disease after the remission. No second relapse was observed during the period of experimental clinical observation (Fig. 1A). The group of linPLP (control) developed severe EAE disease with overall disease burden (AUC of 75.9±44.4), maximal disease deficits (MMS of 4.4±1.4) and dDO at 8.1±1.7 days (Fig. 1B-D). Importantly, 3/9 control mice died within the acute phase of EAE (up to day 16) and 89 % (8/9) of the mice reached or exceeded score 3 (Fig. 1E), all signs of a highly severe EAE. However, mice immunized with the cPLP developed minimal clinical disease with significantly low overall disease burden (AUC=22.1±16.4, p=0.031 student's *t*-test), very low MMS (1.3±0.9, p<0.0001) and significantly delayed disease onset (dDO=12.4±2.9, p=0.0011; Fig. 1B-D). In the same direction, no mice died acutely in cPLP group (p=0.052, Kaplan-Meier survival analysis) and only 1/10 barely reached score 3 (10% or 1/10 of the cyclic group, p=0.0001, Kaplan-Meier survival analysis; Fig. 1E) with the remaining 9/10 having a score between 0 and 2. Overall our data indicate that the cyclization of a linear PLP (in the form of the cPLP peptide) significantly reduces the clinical encephalitogenic properties of the peptide in the recipient animals.
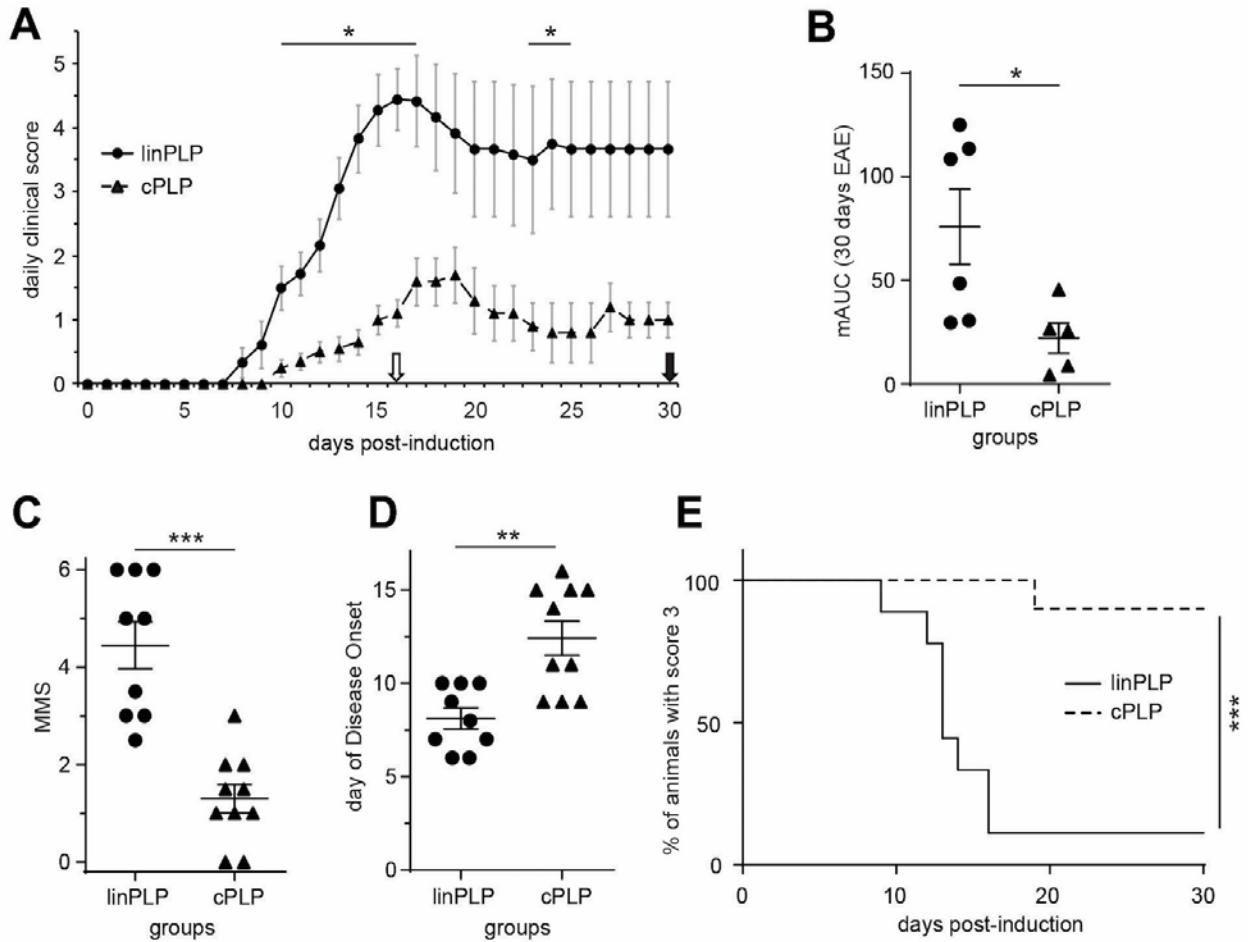
Fig. 1. Clinical course and outcome parameters of animals immunized with linPLP or cPLP. Panel (A) shows the long-term (chronic) clinical course and parameters of the animals; on day 16 (white arrow) animals were sacrificed for the acute phase, on day 30 (black arrow) animals were sacrificed for the chronic phase. The overall burden of disease (mAUC), the maximal disease deficits (MMS, C) and the day of disease onset (D) were significantly better in the cPLP animals. Kaplan-Meier survival analysis for the % of animals reaching severe clinical scores (≥3) showed that animals immunized with cPLP had a mild EAE. Data are displayed as individual values plus mean±SEM. * p<0.05, ** p<0.01, *** p<0.001.

2.2. Cyclic PLP causes a minimal pathology in the spinal cords of the animals compared to its linear analog

In order to study the inflammatory, axonopathic and demyelinating processes in the mice we analyzed the pathology of spinal cords in both acute and sub chronic phases of the disease. During acute phase, the control group had a significant higher inflammatory burden within the spinal cords of the mice. The inflammatory load was at least 300% more in the control group than cPLP group (linPLP=1371.5±517.4/mm^2 and cPLP=439.6±341.7/mm^2, p<0.001; Fig. 2A). Inflammatory foci were also significantly larger with at least 150% more cells in the control group than cyclic group (linPLP=76.7±20.4 and cPLP=31.6±18.5 cells/focus, p<0.001; Fig. 2B). As an indication of less encephalitogenic potential for the

infiltrated cells in the cPLP animals, we also noted a discrepancy between the inflammatory load (InfLoad) and the score of some mice in the cPLP group (>350cell/mm^2 with clinical score of 1), while linPLP mice with a similar InfLoad (>350cells/mm^2) had a clinical score ≥3. In addition to more inflammation in acute phase, the linPLP group had significant more axonal injury than cPLP group (Fisher's Exact chi-square p<0.001; Fig. 2D,H,I) and more demyelination (linPLP=2.7±0.8% and cPLP=0.7±0.4% of spinal cord white matter, p<0.05; Fig. 2C,F,G). Spheroid and ovoids of axons, which indicate the presence of axonotmesis, were only present in the linPLP group and completely absent from the cPLP one (only some scattered dystrophic axons). Similarly, axonal density was significant reduced in linPLP compared to cPLP group (Fisher's Exact chi-square p<0.001, Fig. 2E,H,I). Additional and most important are the observations that the axonal and myelin integrity and density in cyclic group were well preserved even in areas of spinal cord with presence of many inflammatory cells (Fig. 2I), whilst control group had injured and lost axons in almost every area adjacent to inflammatory foci (Fig. 2H).

Sub chronic phase of the disease had no differences between the surviving mice of the 2 groups concerning the inflammatory load within their spinal cords (linPLP=74.3±49.1/mm^2 and cPLP=82.4±35.4/mm^2, p=0.398) and the size of the inflammatory foci (linPLP=18.4±10.0 and cPLP=13.3±6.0 cells/focus, p=0.254). Axonal pathology (injury and axonal loss) and % demyelination (0.2±0.04% and 0.1±0.02% for linPLP and cPLP respectively) were also similar between the surviving mice of the 2 groups (p>0.05, supplementary table). However, these results must be dealt with critical cautiousness since they represent pathology of mice in the control group that survived the acute phase of their disease and had milder clinical scores (selection bias due to severe EAE and consequent mortality in the linPLP group).
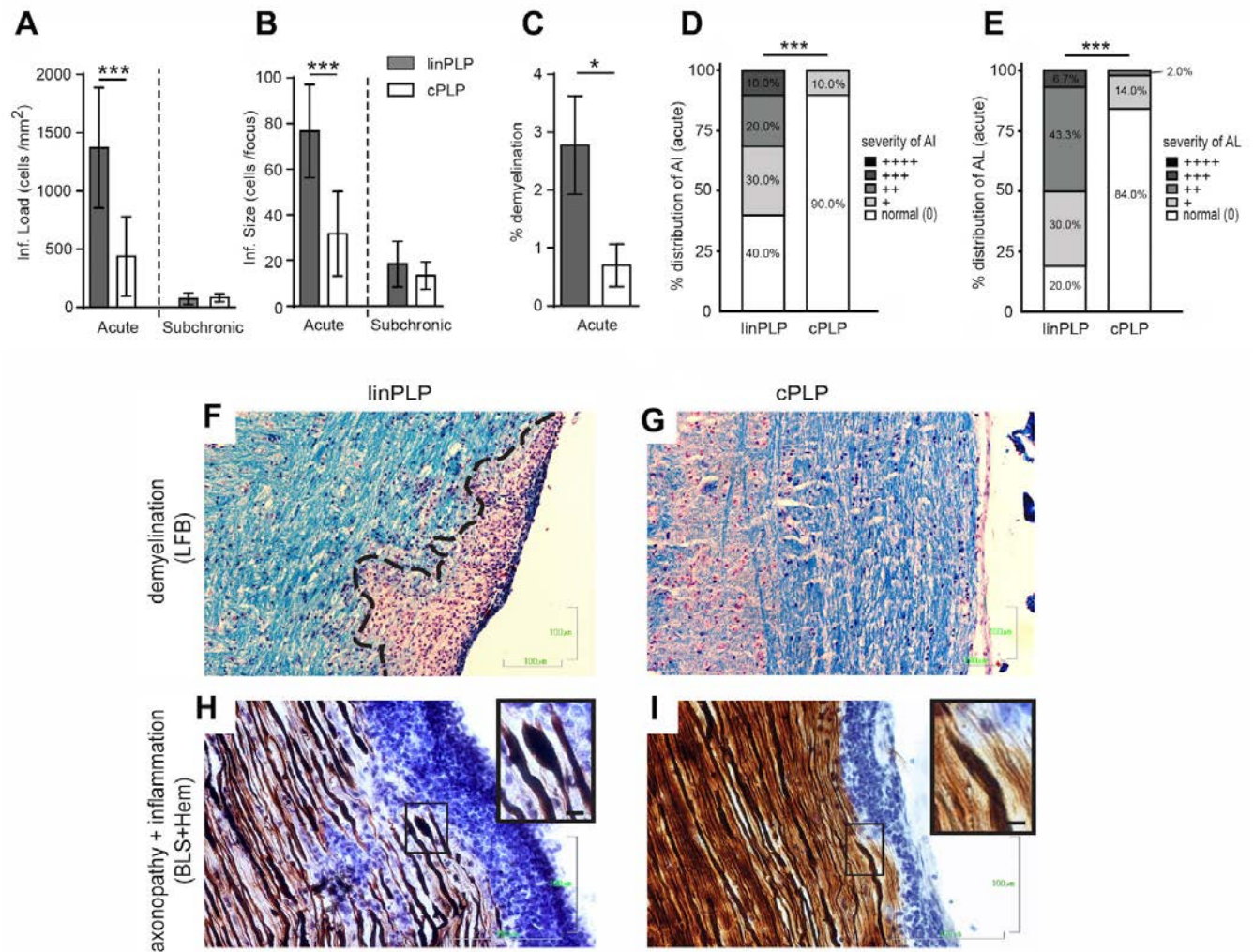
Fig. 2. LinPLP induced very mild encephalitogenic processes in the spinal cords of the immunized animals. Inflammatory load (Inf. Load per mm^2, A) and size of inflammatory foci (Inf. Size, B) were significantly lower in acute phase of cPLP animals; on sub chronic phase inflammatory processes did not differ due to selection bias (see text). Demyelination (C) and axonopathic processes (% distribution of axonal injury, D, and axonal loss, E) were also significantly milder in cPLP animals compared to linPLP during the acute phase, suggesting lower degenerating capacities from the infiltrating cells. Pictures F and G show representative longitudinal spinal cord sections (20x) of linPLP and cPLP immunized animals stained with LFB (blue: intact myelin, red: cell nuclei; dotted outline in F marks the demyelination). Photos H and I show sections (40x) of linPLP and cPLP animals stained with Bielschowsky and Hematoxylin (BLS+Hem, evaluation of axonopathy and inflammation; blue: cells bodies, dark brown: axons); insert in H shows magnification of a spheroid/ovoid adjacent to inflammatory cells (linPLP group) while insert in G shows an intact thick axon next to inflammatory cells (cPLP group). Data are displayed as mean±SEM. * denotes p<0.05, *** p<0.001.

2.3. Cyclic PLP is less mitogenic/immunogenic than linear PLP

The *in vitro* stimulation assays of lymph node cells (LNCs) from linPLP and cPLP mice indicate significantly lower mitogenic/stimulatory effects of the cPLP on the lymphocytes (LNCs, Figure 3). More specifically, unstimulated cells indicate a similar baseline null proliferation of LNCs; addition of a non-specific pan mitogen (concanavalin A) induces a similarly strong proliferation in the LNCs from both linPLP and cPLP mice (p>0.5), indicating a similar proliferating capacity and intact cell-proliferating mechanisms in both linPLP and cPLP LNCs. Under antigen-specific stimulation of the LNCs with their corresponding specific peptide (cPLP or linPLP), those from cPLP mice respond 2.5-fold weaker than the linPLP ones (p<0.05), indicating a significantly weaker stimulatory capacity of the cPLP peptide compared to its linear analog (Fig. 3A). In the same direction, sera from immunized mice showed no anti-PLP IgG antibody production in cPLP- compared to linPLP-immunized animals (1:200 dilution), which was equivalent to background naïve mouse sera reactivity (Fig. 3B). These data indicate that cyclization of PLP significantly reduces *in vivo* antibody production capacity. Overall, our data suggest that cyclization of the PLP peptide reduces its stimulatory capacity on lymphocytes, which results in less PLP-reactive lymphocytes and less IgG. These data are in accordance to the our previous clinical and neuropathological data [16].
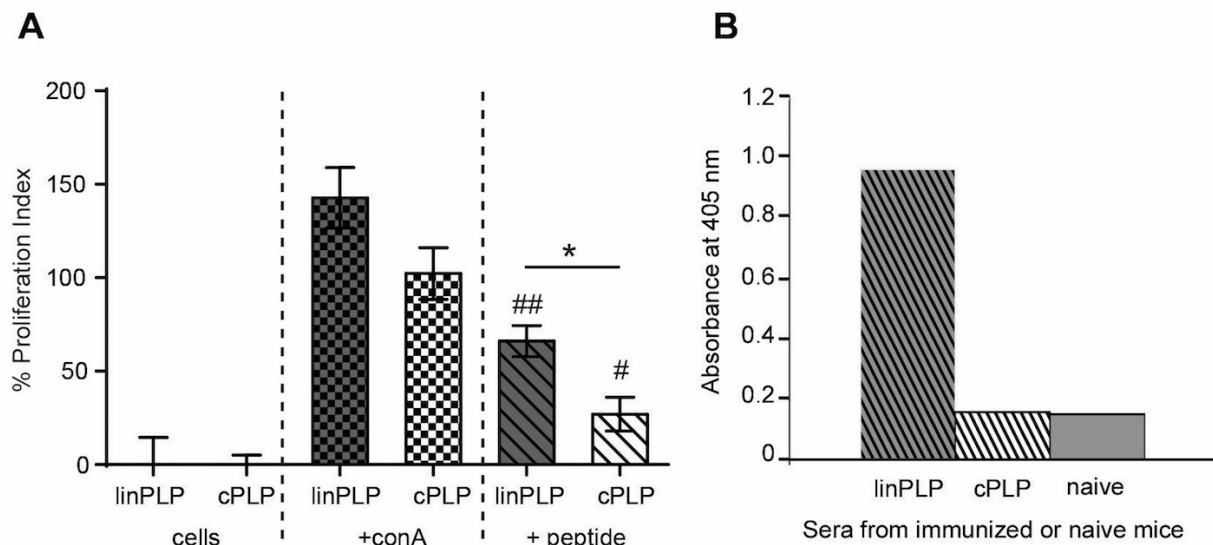

Fig. 3. (A) *In vitro* proliferation assays of lymph node cells from linPLP and cPLP immunized mice. Unstimulated cells (cells) do not proliferate and are used as baseline control. Cells stimulated with the pan-mitogen concanavalin A (+conA) have a similar proliferation potential. Stimulation of the lymph node cells with the cPLP caused a significantly lower proliferation rate compared to linPLP re-stimulation (* p<0.05). # and ## indicates p<0.05 and p<0.01 versus the proliferation of corresponding control cells. (B) IgG levels of serum antibodies at 1:200 sera dilution measured by ELISA following immunization of mice with linPLP and cPLP. Naïve mouse sera was used as a negative background control.

2.4. Binding mode of linPLP$_{139-151}$ and cPLP$_{139-151}$ peptides in complex with murine MHC class II (H2-IA^s)

Previous work has shown that residues L^{145} and P^{148} of linPLP$_{139-151}$ are important for the peptide to bind within the H2-IA^s binding groove, whereas L^{141}, W^{144} and H^{147} are important TCR contact amino acids (Fig. 4A) [23]. Given that the main side chain contact points of peptides interacting with MHC-II alleles occupy positions P1, P4, P6 and P8, linPLP$_{139-151}$ was modeled as such, with S^{140}, L^{141}, G^{142}, K^{143}, W^{144}, L^{145}, G^{146}, H^{147} and P^{148} in allele positions P1-9 respectively. In addition, the electrostatic potential continuum of H2-IA^s was calculated (Fig. 4B) supporting the modelled binding position of the linear peptide, in which P6 appears to be hydrophobic, therefore should accommodate L^{145} and P4 is highly negatively charged suggesting that it is a binding region for the positively charged side chain of K^{143} (Fig. 4B).

As shown in Figure 4C for linPLP$_{139-151}$, the specific electrostatic binding elements to the cavity are hydrogen bonds made by the S^{140} hydroxyl group with T52α in P1 and H^{147} with T56α and strong polar contacts include K^{143} interacting with E74β and D30β in P4 as mentioned previously, as well as D^{149} forming a polar bridge with R76α. The basic hydrophobic contacts represented are L^{145} buried deep in P6 interacting with F11β, F13β and Y32β in a highly hydrophobic region of H2-IA^s and the P^{148} non-polar interactions with Y63β and I72α as it is located between them. Based on this topology of the linear peptide, it is clear that the main potential TCR contact residues are L^{141}, W^{144} and H^{147}, as has been previously reported [23].

In the case of cPLP$_{139-151}$, critical interactions for binding within the cavity of the MHC allele are maintained, such as K^{143} in P4, L^{145} in P6 and P^{148} in P9. These residues maintain their interactions with E74β and D30β (K^{143}), F11β, F13β and Y32β (L^{145}) and Y63β and I72α (P^{148}) (Fig. 4D). However, cyclization does not allow S^{140} to interact with T52α or H^{147} with T56α, neither D^{149} forms a polar interaction with R76α due to conformational restrictions of the cyclization. What is interesting is that the TCR interaction interface in largely changed, with positions P5 and P8 occupied by H^{147} and F^{151} and K^{150} respectively. Even though L^{141} maintains its relative position towards the TCR, W^{144} is somewhat replaced by H^{147} and the most significant change is F^{151} and K^{150} pointing up, thus replacing the role of H^{147} of the linear counterpart in P8 (Figs. 4C, 4D). Hence, the conformational differences underlying the binding elements noted for cPLP vs. linPLP in complex with H2-IA^s may account for the significant different pathological outcomes of the peptides.
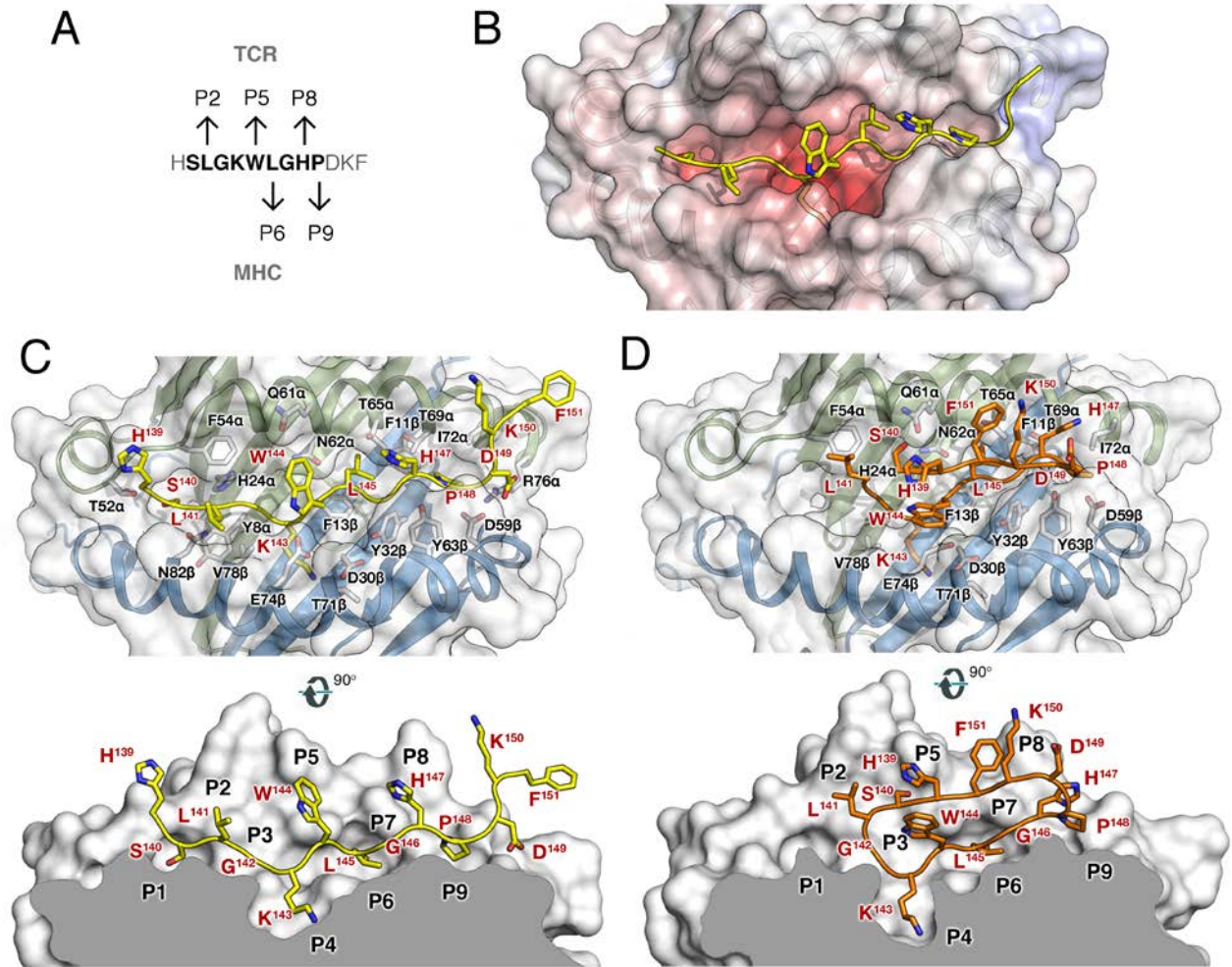
Fig. 4. Computational structural models of linear and cyclic PLP$_{139-151}$. (A) H2-IA^s and TCR contact points for linPLP based on the results by Kuchroo *et al.* [23]. (B) Continuum of electrostatics of the surface for H2-IA^s, performed using APBS (±12 *kT/e*). Red color is for negative and blue for positive, whereas linPLP is depicted in yellow. (C) Mode of linPLP (in yellow) binding to H2-IA^s and (D) mode of cPLP (in orange) binding to H2-IA^s. H2-IA^s chains *α* and *β* are depicted in green and blue color respectively. Peptide labels appear in red, H2-IA^s in black and van der Waals surface is shown in white color.

3. Conclusion

The present experimental study indicates a reduced encephalitogenic effect of cPLP peptide compared to its linear analog. Our preclinical and histopathological data of acute phase (highest disease activity) converge to the fact that cPLP is less potent in causing tissue damage and a consequent of clinical disease. Of special interest is that mice from both groups with similar inflammatory burden in their spinal cords displayed different clinical severity scores depending on whether they were immunized with the linear or the cyclic peptide (very low scores in the cPLP animals and severe score in the linPLP ones). This is in agreement to the *in vitro* restimulation data of LNCs, which confirmed the lower stimulatory effects of cPLP compared to the linPLP peptide, and to the reduced *in vivo* anti-IgG PLP antibody production

in cPLP-immunized animals compared to linPLP. These data collectively indicate that the cyclization of a linear encephalitogenic peptide reduces the activation of lymphocytes and their specificity to their antigenic targets in the CNS tissue.

The minimal clinical, immunogenic and tissue pathology induced by the cyclic peptide could be theoretically explained by its intracellular processing and breaking into linear peptides following its uptake from the antigen-presenting cells. Previous studies from our group with other cyclic peptides indicate that despite higher stability of a cyclic peptide to lysosomal enzymes versus its linear analog, it can still produce degradation by-products that can have a residual activatory potential on lymphocytes [27-30]. This mechanism could be responsible for the observed mild clinical disease and pathology but it is not capable to induce the complete spectrum and severity of the linear peptide. The similar residual inflammatory, demyelinating and axonopathic processes of subchronic phase should be cautiously viewed under the spectrum of high selection bias in the linPLP group (due to mortality) that has removed from the longer follow-up the more severely affected mice. Evidently, the degradation by-products could also probably explain a relatively high cPLP potential (equal to linPLP) to induce *in vitro* IFN-gamma secreting T-lymphocytes, as we showed previously [16], although these cells seem less primed to target the correct (i.e. linear) peptide *in vivo* and cause the maximum of tissue damage.

The modeling studies suggest that linear and cyclic PLP$_{139-141}$ peptides share similar conformational profiles when it comes to MHC binding but more importantly, very different profiles in regards to potential TCR recognition and interaction sites, which is supported by other studies [23]. More specifically, for linPLP, primary TCR contacts are L^{141}, W^{144} and H^{147} at positions P2, P5 and P8 respectively (Fig. 4C), in contrast to cPLP, where L^{141} is maintained in P2, but H^{147} is localized in P5 and F^{151} and K^{150} occupy P8. This differentiation in the topology of peptide TCR contacts gives insights into the likely mechanisms regarding the different pathological and immunological outcomes noted in SJL/J mice.

Most importantly, the present data with the cPLP peptide in SJL/J mice are in complete agreement to our previous findings with a cMOG peptide in another mouse strain (C57BL/6 mice) [26], suggesting that the concept of a peptide-cyclization is valid in different strains and conditions. As the cyclization concept could be applied in other strains and peptides as well, we provide for the first time the proof-of-concept for a novel future therapeutic regime of multiple autoimmune disorders (not only CNS-related but with other organ-targets) on a peptide-, disease- and patient-selective basis.

4. Experimental section

4.1. Solid phase peptide synthesis of linear and cyclic PLP$_{139-151}$

The synthesis of linear PLP$_{139-151}$ (linPLP) and cyclo(139-151) PLP$_{139-151}$ (cPLP) peptides, H^{139}SLGKWLGHPDKF^{151} (rat, mouse) were synthesized at ELDrug SA (Patras Science Park, Greece) (Fig. 5) [31, 32]. Following assessment using analytical HPLC and mass spectroscopy (ESI-MS) peptides were shown to be > 98 % pure as we previously published [16].
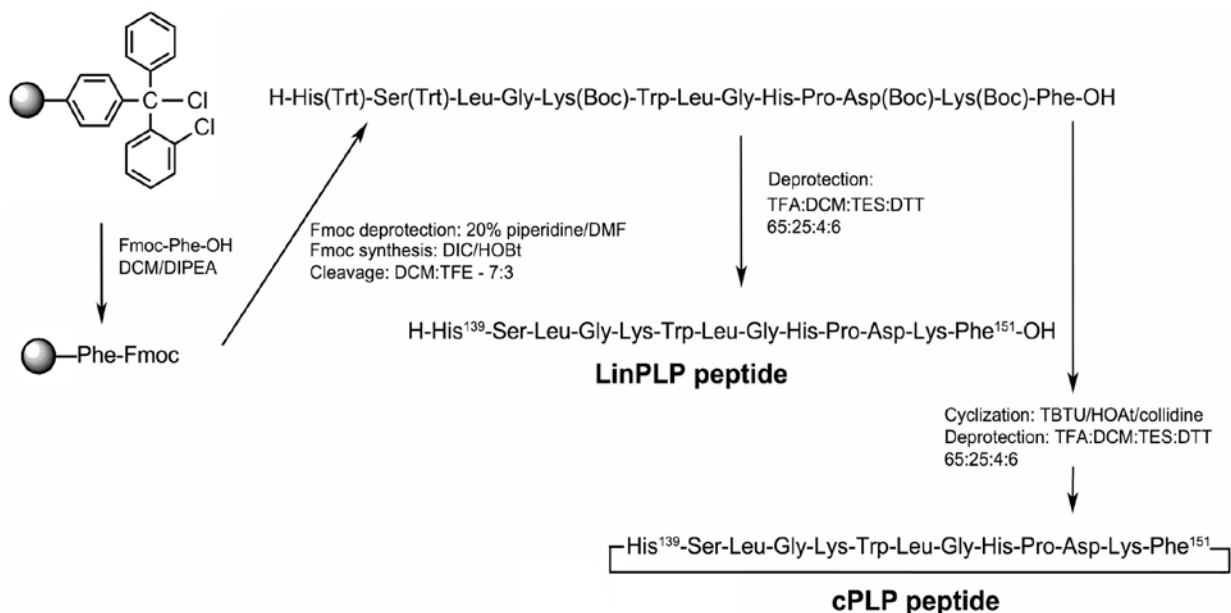
Fig. 5. Synthetic procedure for linear and cyclic PLP peptides

4.2. Animal handling

Female SJL/J mice, 8 weeks-old, were purchased from Hellenic Pasteur Institute, Athens, and housed in the P3 animal facility of the B' Neurological Department of the AHEPA University Hospital, Aristotle University Medical School, Greece. Animals were handled in accordance with the National Institute of Health guidelines, were fed a regular diet and given water without antibiotics.

4.3. Experimental groups and induction of EAE.

Animals were randomly divided into 2 experimental groups: 1) the control group which received the linear PLP$_{139-151}$ (linPLP, n=9), and 2) the cyclic-PLP$_{139-151}$ group (cPLP, n=10) which received the corresponding cyclic PLP$_{139-151}$ peptide. EAE was induced in SJL/J mice using a common vaccination scheme but each animal received the corresponding peptide (linPLP or cPLP) according to its group. Briefly, on day 0 (day of disease induction) each mouse received subcutaneously (sc) 150 µg of the respective PLP$_{139-151}$ peptide (linear or cyclic) in its hindlimb plantar. The peptides were diluted in 50 µl of PBS and were emulsified with 50 µl of CFA (8 mg/ml *Mycobacterium Tuberculosis* HR37a in Incomplete Freund's Adjuvant) per animal, thus producing an emulsion of 100 µl final volume per animal. On the same day (day 0), each mouse received additionally 400 ng pertussis toxin intraperitoneally (ip), dissolved in 500 µl filtered PBS. On day 2 animals received an ip booster of pertussis toxin (200 ng pertussis toxin dissolved in 500 µl filtered PBS per animal).

Animals were daily evaluated for clinical signs of disease, starting from day 1 post immunisation, using a 6-grade clinical scale, as previously described [26, 33]: 0= normal animal, 1= inability to elevate the tail above the horizontal level, 2= flail tail, 3= score 2 plus inability to turn from supine to prone position, 4= score 3 plus paresis or paralysis of hind limbs, 5= score 4 plus paresis of front limbs, 6= death from EAE. Moreover, animals were daily weighted throughout the entire experimental period to evaluate body weight loss due to the induced disease.

4.4. Histopathology

Animals were humanly sacrificed under deep anaesthesia at acute phase of the disease (day 16) and at a sub chronic phase (day 31) of their disease. Their clinical scores at the days of sacrifices were recorded and used for correlations. All animals were transcardially perfused with ice cold PBS (approximately 30 seconds) followed by ice cold 4% paraformaldehyde in PBS (4% PFA) for 5 minutes. Brains and spinal cords were removed, post-fixed overnight in 4% PFA, cryoprotected by incubation for 3-4 days in 30% sucrose and then routinely processed for sagittal or longitudinal cryostat sectioning at 6 µm. Due to prevalence of inflammatory, axonopathic and demyelinating processes in the spinal cords of the animals, all relative histopathological studies were focus in spinal cords.

Axonal and inflammatory pathology were studied on longitudinal spinal cord sections stained with a modified Bielschowsky silver impregnation method combined with Haematoxylin counterstaining, as we previously established [26, 33, 34]. Evaluation of axonopathy and inflammatory burden was performed under a light microscope (Olympus Axioplan-2) by 2 group-blinded evaluators on 3 different longitudinal spinal cord sections spaced approximately 100 µm apart. Using previously established semi-quantitative scales [26, 33], axonal pathology was evaluated under high power (40x) observation. Axonal injury (AI) was evaluated using a 0-4 semi quantitative scale [26] (0 = no AI, 1+ = scattered dystrophic injured axons without any spheroid or ovoid, 2+ = mild AI with the presence of at least one spheroid or ovoid, 3+ = moderate AI, 4 + = severe AI). Injured axons were either identified as spheroids and ovoids (which represent axonotmesis) or dilated (dystrophic) axons which represent injured axons not yet being cut. Axonal loss (AL) was evaluated using the following scale [0 = normal axonal density, 1+ = increased interaxonal distances (<25% AL), 2+ = mild AL (26–50%), 3+ = moderate to severe (51–75%) AL, 4+ = severe AL (>75%)]. It is important to note that score of AL "1+" did not represent a true reduction of axons but rather increased interaxonal distances due to tissue oedema, a phenomenon that was reversible after oedema reduction at sub chronic phase. Inflammatory processes were evaluated by the size of inflammatory foci (number of inflammatory cells per perivascular inflammatory foci, "InfSize") and the total inflammatory load of the tissue number of inflammatory cells -perivascular and parenchymal- ("InfLoad"), under 20x optical fields with the aid of a prefrontal grid.

Demyelinating procedures were evaluated on longitudinal sections stained with Luxol fast Blue and counterstained with Nuclear Fast Red using standard protocols [26, 33]. Evaluation was performed on 3 spinal cord sections as described above for axonopathy, under 20x optical fields with the aid of a prefrontal microscope grid: we measured the total (intact and

lesioned) and the demyelinating (lesioned) surface of the spinal cord's white matter for each optical field and then calculated the % percentage of white matter's demyelination (% Dem).

4.5. Immunological assays

4.5.1. Cell proliferation assay

At day 10 post- induction animals of either linPLP or cPLP groups were euthanized with diethyl-ether and their inguinal lymph nodes were extracted. After dissociation of the lymph nodes of each animal on a petri-dish containing a sterile mesh, the cells were collected and washed from tissue debris with two sequential centrifugations (1500 rpm, 10 min) in full growth medium [0.3% 2-mercaptethanol solution (0.1%) (Sigma), 1% 100 mM sodium pyruvate (Gibco), 1% 200 mM glutamine 1 x (Gibco), 5% fetal calf serum (Gibco), 1% penicillin/streptomycin (Gibco), 1% MEM non-essential amino acids 100 x (Gibco) and 90.7% RPMI 1640 with glutamine (Gibco)]. The isolated LNCs were then transferred into 96- well plates at a concentration of 4×10^5 cells per well and incubated in triplicates, in presence of their specific antigens (cyclic or linear PLP peptide, 100 µg/ml/well, specific activation) or unspecific mitogens (1 µg/ml/well ConA, unspecific activation), for 48 hours at 37°C and 5% CO_2. Plain LNCs from linPLP or cPLP groups (without any addition) were used as controls (baseline mean proliferation rhythm of the cells).

Following the incubation of 48 hours, viability and proliferation of lymphocytes were evaluated using the 3-4,5-dimethylthiazol-2-yl-2,5-diphenyltetrazolium bromide (MTT) proliferation assay, according to manufacturer instruction (R&D Systems). Results of optical absorbance (OD) of each well were obtained using a spectrophotometer at 540nm and were used for calculation of % cell proliferation [= mean OD of the corresponding wells / OD of unstimulated LNCs) *100].

4.5.2. Antibody ELISA assay

Blood was collected and sera was isolated from mice prior to and 4 weeks after immunization with CFA. linPLP$_{139-151}$ and cPLP$_{139-151}$ peptides were conjugated to BSA and coated onto polyvinyl chloride (PVC) microtiter plates at 10 µg/ml in 0.2 M $NaHCO_3$ buffer, pH 9.6, O/N at 4° C. Non-specific binding was blocked with 2% BSA for 1 hour at room temperature. Following washing of plates with 0.05% Tween 20/PBS, 1/200 dilutions of sera were added and incubated for a further 2 hours at room temperature after which bound antibody was detected using HRP-conjugated sheep anti-mouse antibody (1/1000 dilution in PBS) (Amersham, UK) and developed using 2,2'-azino-di(3-ethylbenzthiazoline)6-sulfonic acid (ABTS) (Sigma, UK). Absorbance at 405nm was read using a Fluostar Optima microplate reader (BMG labtech, Offenburg, Germany).

4.6. Statistical analysis

Statistical analysis of the data was performed using the SPSS 23.0 and GraphPad Prism 6 software. Scale clinical, histopathological and *in vitro* proliferation data were initially

tested for normality using Shapiro-Wilk test to assess their validity for parametric analysis (Student's t-test). For non-parametric analysis of two groups we used the Mann-Whitney U test. For comparison of nominal or ordinal data we applied a Pearson chi-square test or Fisher's exact test, depending on the tables' properties. Animals that died due to EAE (score 6) were mathematically kept within their group until end of follow-up to avoid masking of the true clinical group condition and thus confer data bias. The total disease burden (evaluated as the area under the curve, AUC), the maximal disease severity (evaluated as the mean maximal score, MMS) and the day of disease onset (mean day of disease onset with a clinical score of 1, dDO) for each group were calculated as previous described in detail [26, 35]. Survival analysis was performed using Mantel-Cox log-rank test (Kaplan-Meier survival analysis). Values are expressed as mean±SE. For antibody assays, mean values were compared using the Student's two-tailed *t*-test. P value threshold indicates a statistically significant difference where, of * $p<0.05$, ** $p<0.01$, *** $p<0.001$

4.7. Computational models of linear and cyclic PLP$_{139-151}$ peptides in complex with murine H2-IA^s

The H2-IA^u complex, comprising of the MBP$_{1-11}$ peptide crystal structure (PDB ID: 1k2d; 2.20 Å resolution) [36] was used as a template for the H2-IA^s complex homology model as in previous studies [37]. The primary sequence of the two chains were obtained from the Universal Protein Resource (UNIPROT) database (UNIPROT IDs: P14437.1 and P06345.1 respectively). The homology model was built using MODELLER v9.7 [38] and the construction involved the disulfide bonds between C107 - C163 in chain *α* and C15 – C79 and C117 – C173 in chain *β*. The overall stereochemical quality of the final model was evaluated by the discrete optimized energy (DOPE) and thorough visual inspection. The linear peptides were docked in the cleft by means of structural alignment according to previous studies [23]. The cyclic peptide (cPLP) was constructed via manual N- and C-terminal bonding of the linear peptide following energy minimization using the conjugate gradient algorithm. Electrostatic surface calculations on H2-IA^s were performed using PDB2PQR [39] to prepare the protein and Pymol APBS default settings [40].

Acknowledgements

Author contributions

AL designed and performed EAE experiments, acquired and/or analyzed clinical/histology/T-cell data and wrote the manuscript. AG and RL were involved in EAE and

T-cell experiments; MK and VA acquired and analyzed the antibody data. M-TM performed the computational studies and GD synthesized the peptides. NG, JM and VA discussed the project, provided intellectual input, planned experiments, wrote and edited the manuscript and supervised all staff.

References

[1]   N. Grigoriadis, T. Ben-Hur, D. Karussis, I. Milonas, Axonal damage in multiple sclerosis: a complex issue in a complex disease, Clin Neurol Neurosurg, 106 (2004) 211-217.

[2]   A. Ben-Nun, I.R. Cohen, Experimental autoimmune encephalomyelitis (EAE) mediated by T cell lines: process of selection of lines and characterization of the cells, J Immunol, 129 (1982) 303-308.

[3]   V.K. Kuchroo, R.A. Sobel, T. Yamamura, E. Greenfield, M.E. Dorf, M.B. Lees, Induction of experimental allergic encephalomyelitis by myelin proteolipid-protein-specific T cell clones and synthetic peptides, Pathobiology, 59 (1991) 305-312.

[4]   S. Zamvil, P. Nelson, J. Trotter, D. Mitchell, R. Knobler, R. Fritz, L. Steinman, T-cell clones specific for myelin basic protein induce chronic relapsing paralysis and demyelination, Nature, 317 (1985) 355-358.

[5]   J.M. Greer, V.K. Kuchroo, R.A. Sobel, M.B. Lees, Identification and characterization of a second encephalitogenic determinant of myelin proteolipid protein (residues 178-191) for SJL mice, J Immunol, 149 (1992) 783-788.

[6]   J.M. Greer, R.A. Sobel, A. Sette, S. Southwood, M.B. Lees, V.K. Kuchroo, Immunogenic and encephalitogenic epitope clusters of myelin proteolipid protein, J Immunol, 156 (1996) 371-379.

[7]   V.K. Tuohy, Z. Lu, R.A. Sobel, R.A. Laursen, M.B. Lees, Identification of an encephalitogenic determinant of myelin proteolipid protein for SJL mice, J Immunol, 142 (1989) 1523-1527.

[8]   M. Degano, K.C. Garcia, V. Apostolopoulos, M.G. Rudolph, L. Teyton, I.A. Wilson, A functional hot spot for antigen recognition in a superagonist TCR/MHC complex, Immunity, 12 (2000) 251-261.

[9]   M. Kalbus, B.T. Fleckenstein, M. Offenhausser, M. Bluggel, A. Melms, H.E. Meyer, H.G. Rammensee, R. Martin, G. Jung, N. Sommer, Ligand motif of the autoimmune disease-associated mouse MHC class II molecule H2-A(s), Eur J Immunol, 31 (2001) 551-562.

[10]   L. Kappos, G. Comi, H. Panitch, J. Oger, J. Antel, P. Conlon, L. Steinman, Induction of a non-encephalitogenic type 2 T helper-cell autoimmune response in multiple sclerosis after administration of an altered peptide ligand in a placebo-controlled, randomized phase II trial. The Altered Peptide Ligand in Relapsing MS Study Group, Nat Med, 6 (2000) 1176-1182.

[11]   S.W. Brostoff, D.W. Mason, Experimental allergic encephalomyelitis: successful treatment in vivo with a monoclonal antibody that recognizes T helper cells, J Immunol, 133 (1984) 1938-1942.

[12]   L. Steinman, J.T. Rosenbaum, S. Sriram, H.O. McDevitt, In vivo effects of antibodies to immune response gene products: prevention of experimental allergic encephalitis, Proceedings of the National Academy of Sciences of the United States of America, 78 (1981) 7111-7114.

[13]   M.K. Waldor, S. Sriram, R. Hardy, L.A. Herzenberg, L.A. Herzenberg, L. Lanier, M. Lim, L. Steinman, Reversal of experimental allergic encephalomyelitis with monoclonal antibody to a T-cell subset marker, Science, 227 (1985) 415-417.

[14]   M. Katsara, G. Deraos, T. Tselios, J. Matsoukas, V. Apostolopoulos, Design of novel cyclic altered peptide ligands of myelin basic protein MBP83-99 that modulate immune responses in SJL/J mice, Journal of medicinal chemistry, 51 (2008) 3971-3978.

[15]   M. Katsara, G. Deraos, T. Tselios, M.T. Matsoukas, I. Friligou, J. Matsoukas, V. Apostolopoulos, Design and synthesis of a cyclic double mutant peptide (cyclo(87-99)[A91,A96]MBP87-99) induces altered responses in mice after conjugation to mannan: implications in the immunotherapy of multiple sclerosis, Journal of medicinal chemistry, 52 (2009) 214-218.

[16]   M. Katsara, S. Deraos, T.V. Tselios, G. Pietersz, J. Matsoukas, V. Apostolopoulos, Immune responses of linear and cyclic PLP139-151 mutant peptides in SJL/J mice: peptides in their free state versus mannan conjugation, Immunotherapy, 6 (2014) 709-724.

[17]   M. Katsara, J. Matsoukas, G. Deraos, V. Apostolopoulos, Towards immunotherapeutic drugs and vaccines against multiple sclerosis, Acta Biochim Biophys Sin (Shanghai), 40 (2008) 636-642.

[18]   M. Katsara, G. Minigo, M. Plebanski, V. Apostolopoulos, The good, the bad and the ugly: how altered peptide ligands modulate immunity, Expert Opin Biol Ther, 8 (2008) 1873-1884.

[19]   M. Katsara, E. Yuriev, P.A. Ramsland, G. Deraos, T. Tselios, J. Matsoukas, V. Apostolopoulos, A double mutation of MBP(83-99) peptide induces IL-4 responses and antagonizes IFN-gamma responses, Journal of neuroimmunology, 200 (2008) 77-89.

[20]   M. Katsara, E. Yuriev, P.A. Ramsland, G. Deraos, T. Tselios, J. Matsoukas, V. Apostolopoulos, Mannosylation of mutated MBP83-99 peptides diverts immune responses from Th1 to Th2, Mol Immunol, 45 (2008) 3661-3670.

[21]   M. Katsara, E. Yuriev, P.A. Ramsland, T. Tselios, G. Deraos, A. Lourbopoulos, N. Grigoriadis, J. Matsoukas, V. Apostolopoulos, Altered peptide ligands of myelin basic protein (MBP87-99) conjugated to reduced mannan modulate immune responses in mice, Immunology, 128 (2009) 521-533.

[22]   M.K. Keramida, T. Tselios, E. Mantzourani, K. Papazisis, T. Mavromoustakos, C. Klaussen, G. Agelis, S. Deraos, I. Friligou, H. Habibi, J. Matsoukas, Design, synthesis, and molecular modeling of a novel amide-linked cyclic GnRH analogue cyclo(4-9)[Lys4,D-Trp6,Glu9]GnRH: stimulation of gonadotropin gene expression, Journal of medicinal chemistry, 49 (2006) 105-110.

[23]   V.K. Kuchroo, J.M. Greer, D. Kaul, G. Ishioka, A. Franco, A. Sette, R.A. Sobel, M.B. Lees, A single TCR antagonist peptide inhibits experimental allergic encephalomyelitis mediated by a diverse T cell repertoire, J Immunol, 153 (1994) 3326-3336.

[24]   V.K. Kuchroo, R.A. Sobel, J.C. Laning, C.A. Martin, E. Greenfield, M.E. Dorf, M.B. Lees, Experimental allergic encephalomyelitis mediated by cloned T cells specific for a synthetic peptide of myelin proteolipid protein. Fine specificity and T cell receptor V beta usage, J Immunol, 148 (1992) 3776-3782.

[25]   M.P. Yannakakis, C. Simal, H. Tzoupis, M. Rodi, N. Dargahi, M. Prakash, A. Mouzaki, J.A. Platts, V. Apostolopoulos, T.V. Tselios, Design and Synthesis of Non-Peptide Mimetics Mapping the Immunodominant Myelin Basic Protein (MBP83-96) Epitope to Function as T-Cell Receptor Antagonists, International journal of molecular sciences, 18 (2017).

[26]   A. Lourbopoulos, G. Deraos, M.T. Matsoukas, O. Touloumi, A. Giannakopoulou, H. Kalbacher, N. Grigoriadis, V. Apostolopoulos, J. Matsoukas, Cyclic MOG35-55 ameliorates clinical and neuropathological features of experimental autoimmune encephalomyelitis, Bioorganic & medicinal chemistry, 25 (2017) 4163-4174.

[27] M. Katsara, T. Tselios, S. Deraos, G. Deraos, M.T. Matsoukas, E. Lazoura, J. Matsoukas, V. Apostolopoulos, Round and round we go: cyclic peptides in disease, Current medicinal chemistry, 13 (2006) 2221-2232.

[28] G. Deraos, M. Rodi, H. Kalbacher, K. Chatzantoni, F. Karagiannis, L. Synodinos, P. Plotas, A. Papalois, N. Dimisianos, P. Papathanasopoulos, D. Gatos, T. Tselios, V. Apostolopoulos, A. Mouzaki, J. Matsoukas, Properties of myelin altered peptide ligand cyclo(87-99)(Ala91,Ala96)MBP87-99 render it a promising drug lead for immunotherapy of multiple sclerosis, European journal of medicinal chemistry, 101 (2015) 13-23.

[29] J. Matsoukas, V. Apostolopoulos, H. Kalbacher, A.M. Papini, T. Tselios, K. Chatzantoni, T. Biagioli, F. Lolli, S. Deraos, P. Papathanassopoulos, A. Troganis, E. Mantzourani, T. Mavromoustakos, A. Mouzaki, Design and synthesis of a novel potent myelin basic protein epitope 87-99 cyclic analogue: enhanced stability and biological properties of mimics render them a potentially new class of immunomodulators, Journal of medicinal chemistry, 48 (2005) 1470-1480.

[30] T. Tselios, V. Apostolopoulos, I. Daliani, S. Deraos, S. Grdadolnik, T. Mavromoustakos, M. Melachrinou, S. Thymianou, L. Probert, A. Mouzaki, J. Matsoukas, Antagonistic effects of human cyclic MBP(87-99) altered peptide ligands in experimental allergic encephalomyelitis and human T-cell proliferation, Journal of medicinal chemistry, 45 (2002) 275-283.

[31] K. Barlos, D. Gatos, 9-Fluorenylmethyloxycarbonyl/ tbutyl-based convergent protein synthesis, Biopolymers, 51 (1999) 266-278.

[32] K. Barlos, D. Gatos, S. Koutsogianni, Fmoc/Trt-amino acids: comparison to Fmoc/tBu-amino acids in peptide synthesis, J Pept Res, 51 (1998) 194-200.

[33] A. Lourbopoulos, N. Grigoriadis, R. Lagoudaki, O. Touloumi, E. Polyzoidou, I. Mavromatis, N. Tascos, A. Breuer, H. Ovadia, D. Karussis, E. Shohami, R. Mechoulam, C. Simeonidou, Administration of 2-arachidonoylglycerol ameliorates both acute and chronic experimental autoimmune encephalomyelitis, Brain research, 1390 (2011) 126-141.

[34] A. Lourbopoulos, N. Grigoriadis, C. Symeonidou, G. Deretzi, N. Taskos, E. Shohami, Modified Bielschowsky silver impregnation combined with Hematoxylin or Cresyl Violet counterstaining as a potential tool for the simultaneous study of inflammation and axonal injury in the central nervous system, Aristotle University Med J 34 (2007) 31-39.

[35] K.K. Fleming, J.A. Bovaird, M.C. Mosier, M.R. Emerson, S.M. LeVine, J.G. Marquis, Statistical analysis of data from studies on experimental autoimmune encephalomyelitis, Journal of neuroimmunology, 170 (2005) 71-84.

[36] X.L. He, C. Radu, J. Sidney, A. Sette, E.S. Ward, K.C. Garcia, Structural snapshot of aberrant antigen presentation linked to autoimmunity: the immunodominant epitope of MBP complexed with I-Au, Immunity, 17 (2002) 83-94.

[37] V. Apostolopoulos, G. Deraos, M.T. Matsoukas, S. Day, L. Stojanovska, T. Tselios, M.E. Androutsou, J. Matsoukas, Cyclic citrullinated MBP87-99 peptide stimulates T cell responses: Implications in triggering disease, Bioorganic & medicinal chemistry, 25 (2017) 528-538.

[38] B. Webb, A. Sali, Comparative protein structure modeling using Modeller, Current protocols in bioinformatics, (2014) 5.6. 1-5.6. 32.

[39] T.J. Dolinsky, P. Czodrowski, H. Li, J.E. Nielsen, J.H. Jensen, G. Klebe, N.A. Baker, PDB2PQR: expanding and upgrading automated preparation of biomolecular structures for molecular simulations, Nucleic acids research, 35 (2007) W522-525.

[40] N.A. Baker, D. Sept, S. Joseph, M.J. Holst, J.A. McCammon, Electrostatics of nanosystems: application to microtubules and the ribosome, Proceedings of the

National Academy of Sciences of the United States of America, 98 (2001) 10037-10041.